Title

Heating-Induced Evaporation of Nine Different Secondary Organic Aerosol Types

Journal

Environmental Science and Technology, 49(20)

ISSN

0013-936X

Authors

Kolesar, Katheryn R
Li, Ziyue
Wilson, Kevin R
et al.

Publication Date

2015-10-20

DOI

10.1021/acs.est.5b03038

Peer reviewed

Environmental Science & Technology

Article

pubs.acs.org/est

Heating-Induced Evaporation of Nine Different Secondary Organic Aerosol Types

Katheryn R. Kolesar,[†] Ziyue Li,[‡] Kevin R. Wilson,[§] and Christopher D. Cappa*[,†]

[†]Department of Civil and Environmental Engineering and [‡]Atmospheric Science Graduate Group, University of California, Davis, One Shields Avenue, Davis, California 95616, United States

[§]Chemical Sciences Division, Lawrence Berkeley National Laboratory, One Cyclotron Road, Berkeley, California 94720, United States

Supporting Information

ABSTRACT: The volatility of the compounds comprising organic aerosol (OA) determines their distribution between the gas and particle phases. However, there is a disconnect between volatility distributions as typically derived from secondary OA (SOA) growth experiments and the effective particle volatility as probed in evaporation experiments. Specifically, the evaporation experiments indicate an overall much less volatile SOA. This raises questions regarding the use of traditional volatility distributions in the simulation and prediction of atmospheric SOA concentrations. Here, we present results from measurements of thermally induced evaporation of SOA for nine different SOA types (i.e., distinct volatile organic compound and oxidant pairs) encompassing both anthropogenic and biogenic compounds and O_3 and OH to examine the extent to which the low effective volatility of SOA is a general phenomenon or specific to a subset of SOA types. The observed extents of evaporation with temperature were similar for all the SOA types and indicative of a low effective volatility. Furthermore, minimal variations in the composition of all the SOA types upon heating-induced evaporation were observed. These results suggest that oligomer decomposition likely plays a major role in controlling SOA evaporation, and since the SOA formation time scale in these measurements was less than a minute, the oligomer-forming reactions must be similarly rapid. Overall, these results emphasize the importance of accounting for the role of condensed phase reactions in altering the composition of SOA when assessing particle volatility.

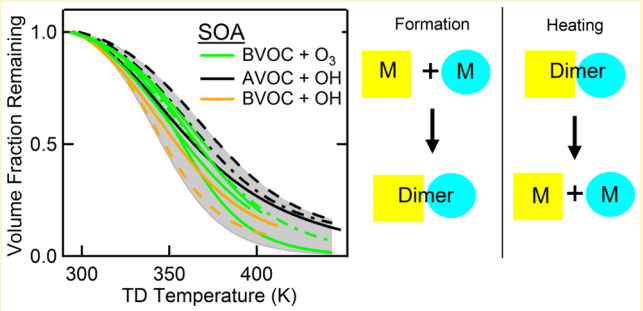

1. INTRODUCTION

Atmospheric particulate matter has an important impact on the Earth's climate[1] and human health.[2] Organic aerosol (OA) is a major component of the total atmospheric particle mass, contributingfrom 20 to 90% of the fine particle mass worldwide.[3] A major portion of OA is secondary organic aerosol (SOA).[4] One pathway for the formation of SOA is when products from the gas-phase oxidation of volatile organic compounds (VOCs) or semivolatile organic compounds (SVOCs) condense onto pre-existing particles or nucleate to form new particles.

Isoprene and monoterpenes ($C_{10}H_{16}$) are two of the dominant biogenic SOA precursors.[5] Near urban areas, additional important sources of SOA include light aromatics, such as toluene,[6] and what are commonly termed semivolatile organic compounds (SVOCs), which are most likely longer chain hydrocarbons that evaporate from primary OA (POA) upon dilution postemission.[7] Whereas isoprene and monoterpenes react readily with O_3 (due to the olefinic carbon−carbon double bonds), aromatics and SVOCs do not. SOA composition and sources consequently vary by location, with generally larger contributions from anthropogenic VOCs (AVOCs) in and around urban areas[8] and larger contributions from biogenic VOCs (BVOCs) in rural areas,[9] although the large variety of sources, compounds, and reaction pathways makes it difficult to accurately predict the spatiotemporal concentration and composition of SOA.

Many laboratory and field experiments have aimed to characterize the yields and chemical composition of anthropogenic and biogenic SOA, using this information to develop parametrizations that can be used in models, from simple box models to complex global models. Nearly all of the commonly used parametrizations, which are generally highly empirical in nature, assume that the gas-particle distribution is well-described through absorptive partitioning theory. However, many studies have shown that SOA particles, especially those formed from the oxidation of terpenoid compounds, can be composed of a large fraction of oligomers.[10−15] It is unclear to what extent the absorptive partitioning-based parametrizations

Received: June 23, 2015
Revised: September 18, 2015
Accepted: September 22, 2015
Published: September 22, 2015

DOI: 10.1021/acs.est.5b03038
Environ. Sci. Technol. 2015, 49, 12242−12252

inherently account for such effects, although most analyses have made no explicit attempt to do so. A commonly used parametrization of SOA formation characterizes the VOC oxidation products as having a distribution of particular volatilities with yields that are VOC-specific. However, although this volatility distribution based framework has provided good fits to SOA formation experiments (e.g., SOA yield versus SOA concentration), the derived effective volatility distributions cannot comprehensively explain observations of particle evaporation in response to either isothermal dilution[16−19] or heating-induced evaporation.[20−23] In particular, they describe SOA that is much too volatile compared to measurements.[21] The presence of oligomers in the condensed phase[10−15] may explain the lower volatility implied by evaporation experiments as oligomers will tend to decrease the overall observable particle volatility when evaporation is probed but may not be well-characterized through growth experiments. Alternatively, the difference could be due to reactions that lead to extensive functionalization of condensed phase species[24] or to diffusion limitations[17,18,25] or could simply indicate an inadequacy of the standard SOA formation models. Regardless, these observations illustrate that there is a clear disconnect between the effective volatility of SOA as characterized by evaporation experiments and that derived from SOA formation studies.

In the current study, the effective volatility of a variety of different SOA types was characterized by heating-induced evaporation in a thermodenuder (TD). The SOA types considered include SOA formed from dark ozonolysis of several BVOCs, α-pinene, β-pinene, *d*-limonene, β-caryophyllene; photooxidation of BVOCs by OH, α-pinene, β-caryophyllene; and photooxidation of several AVOCs, toluene, *o*-xylene, tridecane. The fraction of mass remaining for each SOA type as a function of temperature, referred to as a mass thermogram, was measured, and the particle composition was simultaneously characterized at each temperature using a vacuum ultraviolet aerosol mass spectrometer (VUV-AMS). These measurements, made across a broad suite of different SOA types, establish the extent to which chemical differences between the SOA types do or do not lead to differences in their evaporation behavior. Further, they help to further inform the physical reasons that SOA volatility, when probed via particle evaporation, differs from that derived from SOA growth experiments.

2. MATERIALS AND METHODS

2.1. Secondary Organic Aerosol Generation. SOA was formed in a flow tube from homogeneous nucleation of products from the reaction between individual gas-phase VOCs and an oxidant (either O_3 or OH) around room temperature (~295 K). Each VOC/oxidant reactant pair will be referred to as forming a particular SOA type (Table 1). The experiments were conducted over the period 2009−2014 at the Chemical Dynamics beamline (9.0.2) at the Advanced Light Source (ALS) at Lawrence Berkeley National Laboratory. Different flow tube configurations and types were used depending upon the oxidant identity, the oxidant precursor, and when the experiment was conducted (see the Supporting Information, *SI*). General aspects of all experiments are discussed here.

VOCs were introduced into the flow tube (either quartz or stainless steel) by continuous injection of liquid by syringe pump into a stream of clean, dry N_2. The oxidant or oxidant precursor was added immediately before the flow tube. All O_3 + VOC experiments were conducted in the dark in the absence of an OH scavenger. Experiments in which OH was the oxidant were conducted in the quartz flow tube, which allowed for illumination with four 130 cm long Hg (λ = 254 nm) lamps. OH was produced along the length of the flow tube in two ways: photolysis of O_3 in the presence of water vapor or photolysis of H_2O_2. Although the OH exposure was not directly measured, for the experiments involving O_3 the OH exposure is estimated to be ~1×10^{12} molecules cm^{-3} s based on the measured O_3. The OH exposure for the H_2O_2 experiments is more difficult to estimate but is likely at least an order of magnitude smaller based on previous experiments. The corresponding numbers of oxidation lifetimes for the OH experiments are approximately 6 (toluene), 23 (o-xylene), 14 (tridecane), and 5 (α-pinene), given their respective reaction rate coefficients, although the α-pinene value is particularly uncertain.[26] All photooxidation and ozonolysis experiments were performed in the absence of NO_x (= NO + NO_2) at a relative humidity (RH) of 30%, except for one experiment with β-pinene and O_3 when the RH = 0%.

Table 1. Best-Fit Curves to Experimental Data for Each SOA Type

abbreviation	VOC	oxidant	$S_{VFR} \pm 1\sigma$	$T_{pos} \pm 1\sigma$ (K)
		Biogenic		
αPO_3[a]	α-pinene	O_3	−18.76 ± 1.59	357 ± 3
αPOH	α-pinene	OH[b]	−18.94 ± 3.23	343 ± 3
dβPO_3[c]	β-pinene	O_3	−13.10 ± 2.07	363 ± 4
βPO_3	β-pinene	O_3	−12.93 ± 1.91	354 ± 2
LimO3	*d*-limonene	O_3	−14.63 ± 2.92	364 ± 4
βCO_3	β-caryophyllene	O_3	−13.33 ± 0.54	367 ± 1
βCOH	β-caryophyllene	OH[b]	−14.25 ± 3.17	347 ± 3
		Anthropogenic		
TolOH	toluene	OH[d]	−13.94 ± 3.07	371 ± 4
oXOH	*o*-xylene	OH[d]	−14.05 ± 3.35	363 ± 5
TriOH	tridecane	OH[d]	−10.80 ± 1.02	365 ± 6
LO[a]	lubricating oil	*n.a.*	−30.13 ± 1.19	316 ± 1
average[e]			−14.47 ± 2.54	359 ± 9

[a]Derived from data reported in Cappa and Wilson.[21] [b]H_2O_2 precursor. [c]No active humidification. [d]O_3 precursor. [e]Excluding lubricating oil.

The residence time in the flow tube varied for each experiment based on the experimental setup, although they were generally similar and typically less than 1 min (see the SI). Downstream of the flow tube, residual hydrocarbons and O_3 were removed by passing the airstream through denuders filled with charcoal and Carulite 200 (Carus) catalyst, respectively. Several of the experiments also included a second flow tube downstream of the ozone and charcoal denuders, which was only used for dark "aging" of the SOA for a few minutes. The initial particle mass concentrations for all experiments varied from 400 to 660 μg m^{-3}, assuming a density of 1.2 g cm^{-3}, although they were stable for a given experiment. Although such large concentrations are well-above those observed in the atmosphere, the consistency between different experiments allows for direct comparisons to be made regarding the particle evaporation behavior.

2.2. Thermodenuder. One of two thermodenuders (TDs), consisting of a heated tube followed by a charcoal denuder, was used for each SOA type to induce evaporation. The first was of the same design as described by Huffman et al.,[27] and the second was the TD described in Kolesar et al.[23] The residence time in the fully heated section, $\tau_{res,hot}$, varied from 9.6 to 11.6 s, depending on the experimental conditions; such small

DOI: 10.1021/acs.est.5b03038
Environ. Sci. Technol. 2015, 49, 12242−12252

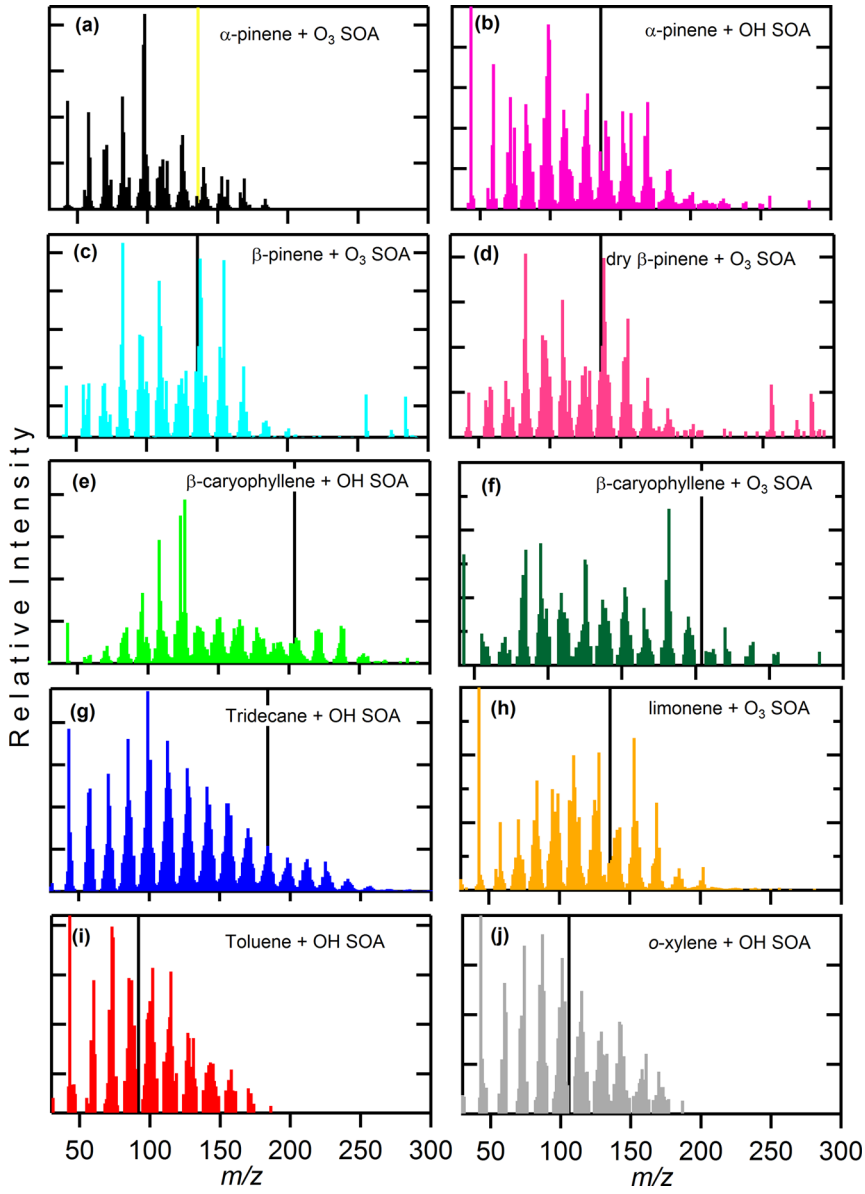

Figure 1. Mass spectra as measured by the VUV-AMS for (a) α-pinene + O_3 SOA; (b) α-pinene + OH SOA; (c) β-pinene + O_3 SOA; (d) dry β-pinene + O_3 SOA; (e) β-caryophyllene + OH SOA; (f) β-caryophyllene + O_3 SOA; (g) tridecane + OH SOA; (h) limonene + O_3 SOA; (i) toluene + OH SOA; (j) *o*-xylene + OH SOA. The m/z corresponding to the molecular weight of the parent VOC is highlighted in black (or yellow for panel (a)).

differences in $\tau_{res,hot}$ are unlikely to have had a substantial influence on the observations (see the SI).[28,29]

2.3. Particle Size Measurements. The extent of aerosol evaporation at a given temperature was characterized by comparing the particle size distribution for particles that passed through the TD to that for particles that passed through the bypass line. Size distributions were measured with a scanning mobility particle sizer (SMPS, TSI Inc.) and were characterized by their volume-weighted median diameter, $D_{p,V}$. The particle volume fraction remaining (VFR) after passing through the TD was calculated as

$$\mathrm{VFR} = \left(\frac{D_{p,V,TD}}{D_{p,V,bypass}}\right)^3 \quad (1)$$

where $D_{p,V,TD}$ is for the TD-treated and $D_{p,V,bypass}$ is for the bypass-sampled distribution. Assuming constant particle density the VFR is equivalent to the mass fraction remaining (MFR), and plots of VFR versus temperature are commonly referred to as mass thermograms. To facilitate quantitative comparison between experiments, each mass thermogram was fit to a sigmoidal curve[30]

$$\mathrm{VFR}(T) = \mathrm{VFR}_{max} + \left(\frac{\mathrm{VFR}_{min} - \mathrm{VFR}_{max}}{1 + \left(\frac{T_{50}}{T}\right)^{-S_{VFR}}}\right) \quad (2)$$

where S_{VFR} characterizes the VFR steepness, and T_{50} is the temperature at which VFR = 0.50. The VFR_{max} is assumed to be unity and VFR_{min} = 0.

2.4. Particle Composition Measurements. Particle composition was characterized online using the time-of-flight (ToF) VUV-AMS at Beamline 9.0.2 at the Advanced Light Source (ALS) at Lawrence Berkeley National Laboratory.[31]

DOI: 10.1021/acs.est.5b03038
Environ. Sci. Technol. 2015, 49, 12242−12252

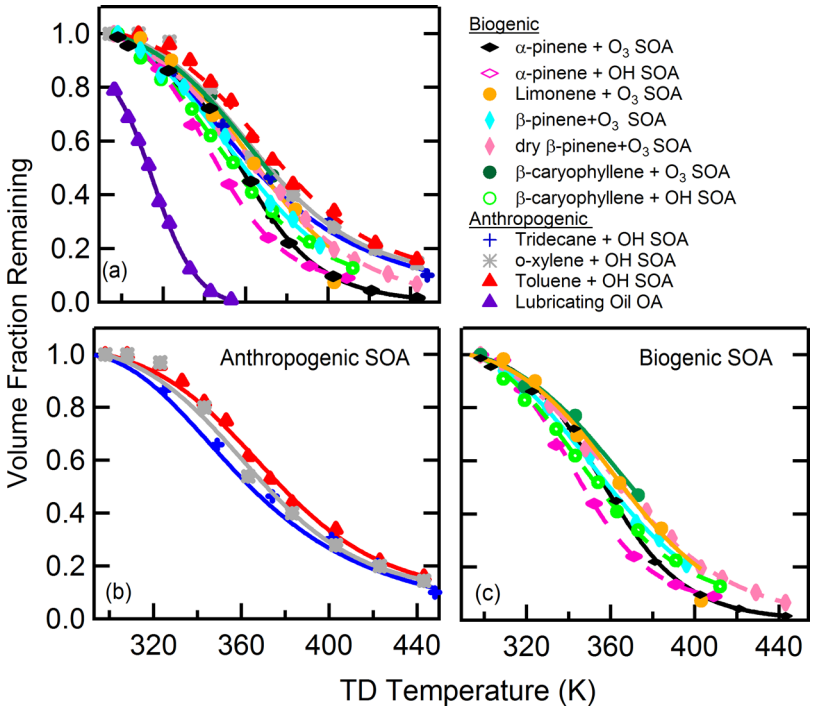

Figure 2. Mass thermograms of OA from this and previous studies. Lubricating oil OA and α-pinene + O_3 SOA are from Cappa and Wilson.[21] Fit lines are determined using eq 1.

Particles were sampled through an aerodynamic lens and directed into a particle beam that impacts a heated block *in vacuo* ($T \sim 120$ °C), which leads to evaporation of the impacted particles. The heated block was designed to allow for particles that "bounce" upon impaction to settle on another heated surface and evaporate. Evaporated molecules were photoionized using 10.5 eV radiation, and the resulting ions were extracted into the ToF mass spectrometer for detection. Background mass spectra were measured directly before each particle composition measurement by sampling the air through a filter, and all reported spectra have been background corrected. The VUV-AMS resolution is $m/\Delta m \sim 2000$, which allows for characterization of the SOA mass spectra with unit mass resolution.

3. RESULTS AND DISCUSSION

3.1. SOA Composition. The VUV-AMS mass spectrum for each SOA type is shown in Figure 1. Differences between SOA types are observed, consistent with each SOA type having a distinct chemical composition.[32−34] The m/z range with observable peaks for a given SOA type is related to the initial number of carbon atoms of the VOC precursor, with the SOA from VOCs with more carbon atoms generally exhibiting peaks out to greater m/z, both for the BVOCs and AVOCs. There are also some differences between the mass spectra for the various monoterpenes (all C_{10} compounds), which likely reflects differences in composition resulting from differences between the reaction rate coefficients and chemical mechanisms associated with terpene reactions with O_3. For example, monoterpene + O_3 reaction rate coefficients are substantially larger (1 to 2 orders of magnitude) for species with endocyclic bonds,[35] and ozonolysis of an endocyclic bond (α-pinene, limonene) results in ring opening; whereas ozonolysis at an exocyclic bond (β-pinene, limonene) results in the formation of two fragments.

Numerous studies[12,36−38] have directly observed dimers and higher order oligomers (>2 monomeric subunits) in SOA formed from the ozonolysis of various VOCs. However, dimers or larger oligomers are generally not observed in the mass spectra obtained from the VUV-AMS, i.e. peaks are not observed at m/z values twice as large as the parent species m/z. The one exception is β-pinene + O_3 (βPO_3) SOA, which exhibits a few distinct peaks in the m/z region where dimers should be found. The lack of dimers in the mass spectrum is generally consistent with measurements of SOA made using the Aerodyne AMS, which tend to show little, if any, signal at $m/z > 100$,[39] although it should be noted that the Aerodyne AMS vaporizes particles at ~600 °C and uses 70 eV electron impact (EI) ionization and thus is not expected to be as "soft" an ionization method as the VUV-AMS. That some techniques show clear evidence of oligomers while others do not likely indicates differences between the measurement techniques and suggests that a use of multiple methods simultaneously to characterize SOA could lead to further refinements in understanding. Most likely, oligomer decomposition during detection (i.e., dissociative photoionization) in both the VUV-AMS and Aerodyne AMS precludes their direct detection. Nonetheless, that there are peaks observed at m/z greater than that of the parent VOC in the VUV-AMS mass spectra indicates that this method is capable of detecting either oxidized monomers directly or large fragments from oligomers in addition to smaller fragments. As such, variations in the absolute and relative intensities of these peaks can provide information regarding chemical changes that occur within the particles with evaporation, as discussed in Section 3.3.

3.2. Bulk Volatility. Mass thermograms for each SOA type have been measured, and the experimental data were fit with eq 2 to determine the S_{VFR} and T_{50} values (Figure 2 and Table 1). The mass thermogram of lubricating oil (LO) from Cappa and Wilson[21] is included for reference. LO particles are liquid and

DOI: 10.1021/acs.est.5b03038
Environ. Sci. Technol. 2015, 49, 12242−12252

are composed of "semivolatile" molecules with C^* values spanning the range of around $0.01-10^4$ $\mu g\ m^{-3}$.[28] The mass thermograms are shown all together (Figure 2a) in addition to being grouped according to VOC type, i.e. as anthropogenic (Figure 2b) or biogenic (Figure 2c). Although there are definite differences between the mass thermograms for individual SOA types, it is also apparent that the mass thermograms exhibit similar general behavior in that they all fall within a relatively narrow range of VFR values at a given temperature and are all much less volatile than LO particles. This suggests that the physical or chemical phenomena responsible for the low apparent volatility are general to all of these SOA types.

The VFR was measured for particles that were passed through the TD at room temperature (RT) for LO and for most SOA types. There is substantial evaporation of LO at RT (VFR(RT) < 1) due to rapid evaporation upon vapor stripping in the charcoal denuder. This is a reflection of the liquid and predominately semivolatile (C^* > 1 $\mu g\ m^{-3}$) nature of LO particles. In distinct contrast, none of the SOA evaporate at room temperature in the TD. Based on recent model results from our group[23] we can conclude that a lack of evaporation at room temperature in the TD indicates that the vast majority of compounds have effective saturation concentrations of $C^* \leq 1$ $\mu g\ m^{-3}$ even though the SOA concentrations were ~500 $\mu g\ m^{-3}$. Thus, none of the SOA types behave as if composed of semivolatile compounds that respond rapidly to vapor stripping in the TD, in conflict with SOA volatility distributions obtained from formation studies.[22,40,41] The time scale associated with the formation of these low-volatility compounds under current experimental conditions must be very short, less than a minute or so based on the residence time in the flow tube where the SOA was formed. Experiments conducted using SOA at much lower mass concentrations (C_{OA} < 20 $\mu g\ m^{-3}$)[23] suggest that these short time scales may be applicable to the ambient atmosphere; however, as the current and these previous experiments were conducted using short formation time scales it will be important for future work to establish the extent to which the formation time scale influences the particle behavior and properties.

These observations are consistent with many other studies, both for laboratory generated SOA[21,42−46] and ambient OA,[20,47] that report no evidence of evaporation at room temperature in TD or volatility tandem DMA (VTDMA) experiments. (Evaporation of SOA at room temperature is known to occur in response to vapor stripping but on much longer time scales.[16,18]) However, in one study by Emanuelsson et al.[30] using βPO_3 SOA, around 30% of the mass (VFR = 0.736 ± 0.083) evaporated at room temperature despite a median residence time of only two seconds in their VTDMA. The reason for this difference between Emanuelsson et al.[30] and both the current study and other literature results is unclear, although it is likely related to details associated with their normalization procedure and not actually evidence of substantial evaporation [Hallquist, M., personal communication].

To facilitate further comparison between the mass thermograms obtained for the different SOA types, the best-fit parameters S_{VFR} and T_{50} are reported (Table 1), along with an average over all the SOA types for which $S_{VFR,avg} = -14.47 \pm 2.54$ and $T_{50,avg} = 359 \pm 9$ K (where the uncertainties are 1σ). The average values characterize the average response of SOA formed under the general experimental conditions (RH = 30% and with no NO_x) to heating-induced mass loss. For comparison, the S_{VFR} for LO is twice that of the SOA average ($S_{VFR,LO} = -30.13 \pm 1.19$) and the T_{50} of LO much lower ($T_{50,LO} = 316 \pm 1$ K, including the evaporation at room temperature); this demonstrates that a wide variety of SOA types are effectively much less volatile than LO.

Although overall the mass thermograms for the different SOA types are generally similar in shape, there are some differences depending on the VOC precursor and oxidant. For example, the T_{50} for the anthropogenic SOA are generally higher than for the biogenic SOA indicating that a higher temperature is required to induce the same mass loss from anthropogenic SOA. Specifically, the average T_{50} for the two groupings ($T_{50,ave,bio.} = 356 \pm 9$K and $T_{50,ave,ant.} = 366 \pm 4$K) are statistically different at the $p = 0.05$ level ($p = 0.046$ for the two-tailed test). The apparently lower volatility of the anthropogenic SOA is in qualitative agreement with results from Loza et al.[48] who found that toluene + OH (TolOH) SOA was lower in volatility than α-pinene + OH (αPOH) SOA and with results from Emanuelsson et al.[49] who observed lower VFR values for TolOH SOA and p-xylene + OH SOA than for αPO_3 SOA at 343 K. The somewhat lower volatility of the anthropogenic SOA might be attributable to heterogeneous "aging" by OH in the flow tube after formation; the number of oxidation lifetimes in the AVOC+OH experiments were generally larger than in the BVOC+OH experiments due to differences in the OH precursors, and the influence of heterogeneous chemistry increases with the number of oxidation lifetimes.[50] Although the T_{50} differed between the anthropogenic and biogenic SOA types, their average S_{VFR} are statistically indistinguishable at the p < 0.10 level ($p = 0.18$ for the two-tailed test). However, despite this statistical indistinguishability, the S_{VFR} values for αP-derived SOA are notably higher than for the other types, which is consistent with differences in previously reported values of the effective enthalpy of vaporization for αPO_3 SOA and TolOH SOA and suggests that this difference is real.[51]

There are further small differences between the mass thermograms for biogenic SOA formed from ozonolysis. In particular, limonene + O_3 ($limO_3$) SOA and β-caryophyllene + O_3 (βCO_3) SOA have the largest T_{50} values, suggesting that they are somewhat less volatile than other types of SOA. This is similar to Lee et al.[46] who found $limO_3$ SOA to be effectively less volatile than αPO_3 and βPO_3 SOA. Unlike the other monoterpenes, since limonene has both an endo- and an exocyclic bond it can react twice with O_3, either in the gas-phase or in the particle-phase after condensation of first generation products.[52] β-Caryophyllene also has two double bonds, suggesting that the reaction of first-generation products leads to a decrease in the effective volatility of the $limO_3$ and βCO_3 SOA types, either due to production of lower volatility monomers or enhancement of oligomers in the condensed phase. There are also small differences between the effective volatility of biogenic SOA depending on the oxidant. For both β-caryophyllene and α-pinene, the SOA from ozonolysis is somewhat less volatile than SOA from OH. This likely reflects differences in the product distributions, both in the gas and particle phases, due to differences in the chemical pathways associated with oxidation by OH versus by O_3. It has been suggested that gas-phase dimers can form from reaction of stabilized Criegee intermediates or secondary ozonides,[52−54] which are only formed from reactions with O_3. Additionally, ozonolysis can lead to the production of very highly functionalized, low-volatility monomer products that do not

DOI: 10.1021/acs.est.5b03038
Environ. Sci. Technol. 2015, 49, 12242−12252

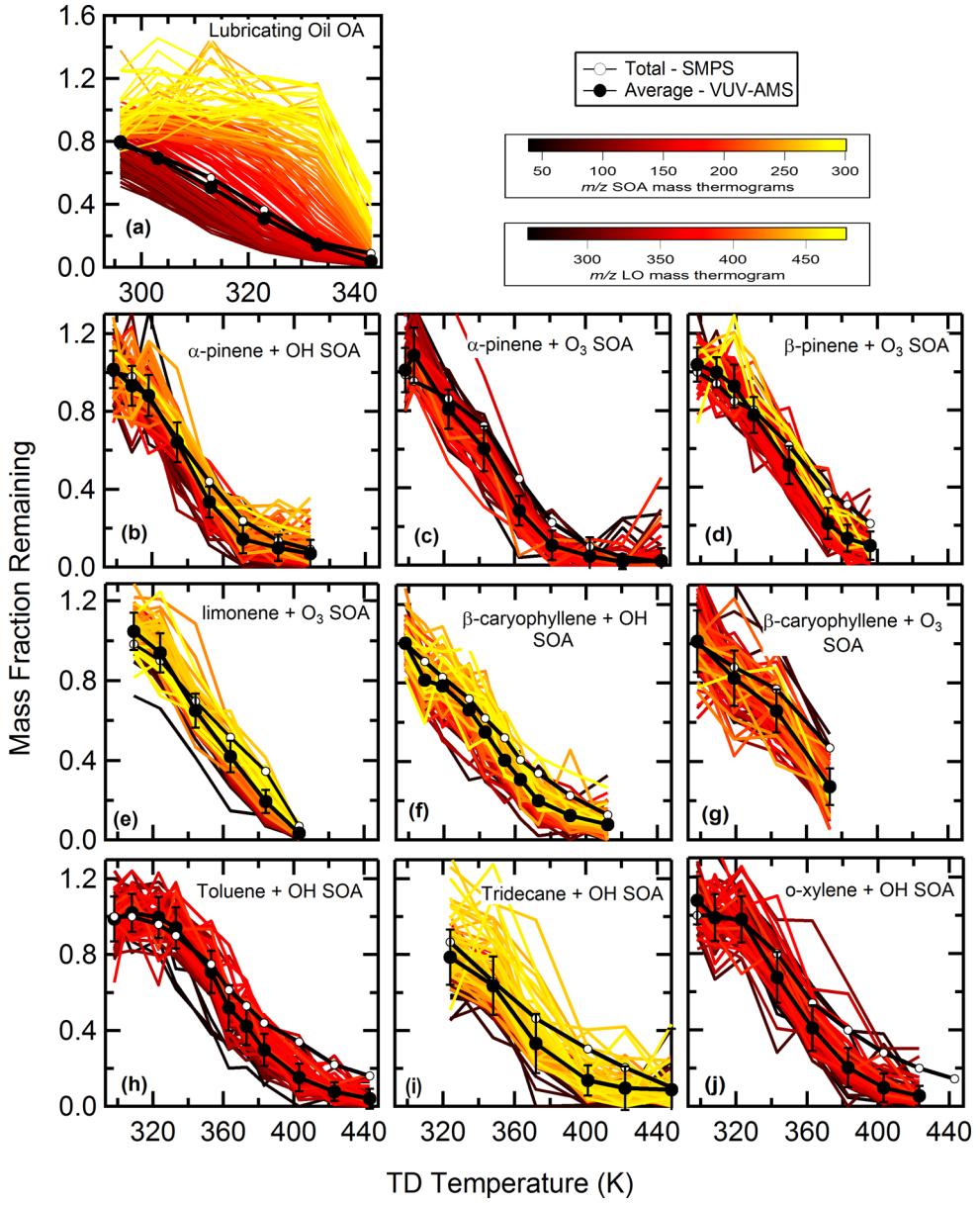

Figure 3. Peak thermograms for every m/z from m/z = 40 to 300 amu for (a) Lubricating oil OA, from Cappa and Wilson (2012); (b) α-pinene + OH SOA; (c) α-pinene + O_3 SOA; (d) β-pinene + O_3 SOA; (e) limonene + O_3 SOA; (f) β-caryophyllene + OH SOA; (g) β-caryophyllene + O_3 SOA; (h) toluene + OH SOA; (i) tridecane + OH SOA; and (j) o-xylene + OH SOA. Line colors indicate the m/z (see color scale). The total mass thermograms (black) for particles from each VOC/oxidant pair from SMPS (open circles) and VUV intensity (filled circles). Panel (a) is a well-mixed liquid. Panels (b)−(g) are SOA from biogenic VOCs, and panels (h)−(j) are SOA from anthropogenic VOCs.

form from reactions with OH.[54] For βPO_3 SOA, an additional experiment was performed with the RH = 0%, as opposed to 30% as in all other experiments. There is no clear difference between the βPO_3 SOA mass thermograms at RH = 0% and 30%, consistent both with observations from both Lee et al.[46] and Emanuelsson et al.,[30] even though RH has been found to influence both the number and mass concentrations of SOA formed for this compound.[55] (The S_{VFR} for the βPO_3 SOA from Emanuelsson et al.[30] actually agrees well with the S_{VFR} reported despite the different room temperature VFR.) The implication is that even though RH can influence the formation and properties of SOA, there is minimal influence on the evaporation behavior.

Overall, our measurements indicate a general similarity of the mass thermograms between different SOA types formed from a wide range of precursor VOCs and oxidants, suggesting that heating-induced evaporation of many SOA types can be reasonably described by a single set of parameters, at least for SOA formed in the absence of NO_x. Likely reasons for this behavior will be examined in the next section.

3.3. Spectral Measurements of Volatility. Mass spectra were measured concurrent with the VFR measurements for each SOA type as a function of temperature. The change in intensity of each peak in the VUV-AMS mass spectrum with temperature, normalized to that observed for the bypass (referred to as a peak thermogram), was determined for each SOA type. Much like the mass thermograms, the peak thermograms exhibit similar behavior across the different SOA types. In general, the intensity of individual peaks all decrease together as temperature increases. This is visually

DOI: 10.1021/acs.est.5b03038
Environ. Sci. Technol. 2015, 49, 12242−12252

apparent by the nearly temperature independent spread in signal intensity and the similarity of the individual peaks to the average behavior. If some compounds (monomers or oligomers) evaporated to a greater extent than others at a given temperature, then the spread of the individual peaks would increase with temperature, as was observed for evaporation of LO particles (Figure 3a).[21] Although individual peaks may derive from multiple compounds, the particular fragmentation patterns that are observed for pure compounds in the VUV-AMS do depend on the unfragmented molecule identity. For example, pinic acid ($C_9H_{14}O_4$; *MW* = 186 amu) and *cis*-pinonic acid ($C_{10}H_{16}O_3$, *MW* = 184 amu), which are known products from α-pinene ozonolysis and photooxidation, both exhibit a clear peak corresponding to the respective parent ion m/z and exhibit distinct fragment peaks with characteristic m/z values.[56] This demonstrates that, to a reasonable extent, the individual peaks represent individual compounds (or fragments thereof). Thus, the similarity in behavior between individual peaks suggests that particle composition—at least as characterized by the VUV-AMS—does not change substantially as the particles evaporate for all SOA types measured here.

These results are consistent with and expand substantially on the results from Cappa and Wilson,[21] who determined peak thermograms for αPO_3 SOA using the same VUV-AMS as here. Additionally, Huffman et al.[57] and Loza et al.[48] both observed minimal changes upon heating to the chemical composition of αPOH SOA and TolOH SOA, as characterized by mass spectra from an Aerodyne AMS, and similar behavior has also been observed for ambient OA.[47] However, Kostenidou et al.[58] report some changes upon heating in the Aerodyne AMS mass spectrum for αPO_3, βPO_3, $limO_3$, and βCO_3 SOA. Specifically, they observed that the signal fraction of m/z 44 ($f44$) increased somewhat with temperature for three of the SOA types (αPO_3, βPO_3, $limO_3$) but was constant with temperature for βCO_3 SOA (although for βPO_3 SOA the $f44$ varied only slightly until the VFR was <0.2). Although compositional variation was assessed based on changes in one peak in the mass spectrum (that reflects, approximately, the oxygen content of the OA), their results nonetheless do indicate a change in the chemical composition of these SOA types upon heating. The reasons that the Kostenidou et al.[58] study gives contrasting results to the current study remain unknown, although it should be noted that their SOA was overall substantially more volatile (T_{50} ~ 330 K) than that observed here and by others.[46]

The current results demonstrate that the results from Cappa and Wilson[21] are quite general for SOA formed under low NO_x conditions and that distillation of individual compounds according to their volatility does not appear to occur upon heating. This, in turn, implies that the particles do not behave as simple, liquid-like mixtures of individual monomeric compounds. This is consistent with measurements of particle "bounce"[59] or estimates of the viscosity of SOA,[60,61] which indicate that SOA often exists as an amorphous, semisolid state. Cappa and Wilson[21] suggested that the constant composition of SOA during evaporation could reflect "layer-by-layer" evaporation from semisolid particles. However, layer-by-layer evaporation would still require that compounds with volatilities much lower than typically observed gas-phase oxidation products were formed originally in high abundances for all of the chemical systems considered here to explain the bulk mass thermogram behavior, i.e. the low effective volatility and generally similar behavior of the various SOA types. Additionally, even if the particles were initially well mixed, heating of the particles should cause the particles to become increasingly less viscous.[62] This would in turn decrease the time scale associated with mixing with the particle, thus leading to, at least in theory, increasingly liquid-like behavior, which was not observed.

Two pathways to exceptionally low volatility compounds in SOA are the formation of oligomers[10−15] and of extremely low-volatility organic compounds (ELVOCs),[54] both of which have been directly measured in SOA particles. ELVOCs will evaporate directly upon heating, while oligomers may decompose or evaporate directly. (If ELVOCs are composed of a substantial number of peroxide bonds,[54] then they may be subject to thermal decomposition as well, which could potentially contribute to particulate mass loss.[63]) Enthalpies of vaporization for individual compounds tend to increase with decreasing vapor pressure,[64] suggesting that direct evaporation of individual low-volatility compounds should be observed as relatively sharp decreases in their particle-phase abundance at specific temperatures.[65,66] Thus, the observed gradual decrease in VFR with temperature would imply that SOA is composed of compounds with a wide range of C^* values (~10^{-10} to 1 $\mu g\ m^{-3}$)[23] if direct evaporation of stable compounds (monomers or oligomers) were driving the behavior. Such compositional changes should have been observed as changes in the VUV-AMS mass spectra with temperature, inconsistent with the observations. Therefore, the condensation of ELVOCs cannot explain all of the experimental observations. Although ELVOCs likely contribute to the formation of many SOA types, their individual volatilities do not dominate bulk particle evaporation. Alternatively, evaporation could have been driven primarily by decomposition of low-volatility oligomers having similar decomposition enthalpies (i.e., temperature sensitivities) and subsequent evaporation of the higher-volatility decomposition products (e.g., monomers). In this case, it is possible to have a multicomponent system for which evaporation does not lead to substantial changes in the residual particle composition, but where the oligomers were formed from monomers that initially had a wide range of individual volatilities.[23] Although there is certainly some preference for certain molecules to form dimers and oligomers[67] and not all oligomers are held together with the same bond types (e.g., hydrogen bonds[15,68] versus covalent bonds[13,69]), if a sufficiently large fraction of the SOA mass is composed of oligomers, then it is reasonable to view the monomeric subunits as being randomly distributed among the possible dimers and oligomers. Consequently, when an oligomer decomposes and the subunits evaporate, or even when an oligomer directly evaporates, the residual SOA composition as observed by instruments that characterize predominately monomeric products or fragments (such as the VUV-AMS used here or the Aerodyne AMS) need not show evidence of substantial changes.

Our observations are complemented by literature measurements for which mass spectra of the evaporating gas-phase species from deposited SOA particles were measured as a function of temperature,[70−72] as opposed to measurements of the residual particle composition after heating (as done here). In these gas-phase measurements, clear differences in the desorption profiles between some of the individual peaks have been observed, and many peaks (including the total signal) exhibit bimodal behavior. For example, Lopez-Hilfiker et al.[70] performed measurements for αPO_3 and αPOH SOA and observed that there were two desorption modes for individual ions identified as structural isomers of pinic and norpinic acid. The effective C^* values associated with the two modes were

DOI: 10.1021/acs.est.5b03038
Environ. Sci. Technol. 2015, 49, 12242−12252

around 0.1 μg m^{-3} and 10^{-6} μg m^{-3}. The C^* value associated with the higher-volatility mode is similar to (although approximately 10−100× smaller than) the monomeric compounds,[73] implying that the lower-volatility mode was attributable to oligomer thermal decomposition. Interestingly, Lopez-Hilfiker et al.[70] observed evaporation of compounds with >10 carbon atoms (the number of carbon atoms in α-pinene), especially at higher temperatures, suggesting that direct evaporation of oligomers can occur concurrent with oligomer thermal decomposition as previously proposed for the SOA concentration-dependent evaporation behavior of αPO_3 SOA.[23] Such a scenario provides a reasonably comprehensive explanation for the apparent low volatility of SOA, the general similarity between mass thermograms for different SOA types, the lack of changes in the VUV-AMS mass spectra with temperature for residual SOA particles, and the multimodal behavior observed for evaporating gas-phase molecules[70,71] and is consistent with previous determinations of large oligomer fractions for SOA.[12,36−38]

4. ATMOSPHERIC IMPLICATIONS

It is increasingly apparent that volatility distributions as derived from typical analyses of particle formation and growth experiments provide an incomplete description of the actual volatility of chemically complex atmospheric SOA particles. The results presented here further demonstrate that this is true for a wide variety of different SOA types formed under zero NO_x conditions. All SOA types were observed to be composed primarily of compounds that have effective volatilities of $C^* \leq 1$ μg m^{-3}, even though the mass concentrations during these experiments were of order 500 μg m^{-3}. Further, it was observed that mass thermograms for the different SOA types (ten in total), formed from the reaction of both biogenic and anthropogenic VOCs with either O_3 and OH, all share general similarities in terms of the temperature sensitivity of evaporation and their overall response to heating. Although some differences between SOA types were observed, likely reflecting compositional differences, overall the generally similar behavior strongly suggests that SOA evaporation is governed by a common process or physical phenomenon. The most comprehensive explanation appears to be that SOA is composed of a substantial fraction of oligomers that decompose upon heating (or dilution).[16,23]

Consequently, there remains a challenge in quantitatively connecting particle formation experiments and their interpretations with evaporation experiments. Clearly, the use of parametrizations such as the 2-product model or the volatility basis set can provide a good fit to the observed SOA formation. However, the derived volatility distributions from these parametrizations do not reflect the effective volatility of the SOA. It is unclear exactly the extent to which this disconnect impacts the simulation of ambient SOA since few efforts[74] have been made to explicitly account for oligomerization in air quality models beyond a simplistic scheme that converts semivolatile SOA to nonvolatile SOA with a time constant of ∼1 day,[75] which is inconsistent with the rapid oligomer formation observed here. The existing SOA parametrizations inherently account for oligomerization to some extent in that the observed SOA levels in growth experiments include the effects of oligomerization. However, since the parameters associated with the formed SOA do not reflect the contributions from oligomers, there can be secondary impacts on simulated SOA in terms of how they respond to dilution or temperature changes. Future work should focus on using integrated, multi-instrument approaches and on developing comprehensive models that can close the gap between observations of SOA formation and evaporation.

■ ASSOCIATED CONTENT

Supporting Information

The Supporting Information is available free of charge on the ACS Publications website at DOI: 10.1021/acs.est.5b03038.

Information detailing the experimental setup configurations for all experiments, including information about particle generation methods and the thermodenuder (PDF)

■ AUTHOR INFORMATION

Corresponding Author

*Phone: 530 752-8180. Fax: 530 752-7872. E-mail: cdcappa@ucdavis.edu.

Notes

The authors declare no competing financial interest.

■ ACKNOWLEDGMENTS

We thank Theodora Nah for experimental assistance and the staff of the ALS for support over the many years these experiments were conducted. This material is based upon work supported by the National Science Foundation under Grant No. ATM-1151062 and by the Atmospheric Aerosols and Health program at UC Davis. The Advanced Light Source is supported by the Director, Office of Science, Office of Basic Energy Sciences, Chemical Sciences Division of the U.S. Department of Energy under Contract No. DE-AC02-05CH1123. K.R.W. is supported by Department of Energy, Early Career Research Program, Office of Basic Energy Sciences, Chemical Sciences Division of the U.S. Department of Energy under Contract No. DE-AC02-05CH11231. This work was performed at Beamline 9.0.2 at the Advanced Light Source at Lawrence Berkeley National Laboratory.

■ REFERENCES

(1) Intergovernmental Panel on Climate Change, *Climate Change 2013: The Physical Science Basis. Contribution of Working Group I to the Fifth Assessment Report of the Intergovernmental Panel on Climate Change*; Cambridge University Press: Cambridge, United Kingdom and New York, NY, USA, 2013; p 1535.

(2) Chen, Y. Y.; Ebenstein, A.; Greenstone, M.; Li, H. B. Evidence on the impact of sustained exposure to air pollution on life expectancy from China's Huai River policy. *Proc. Natl. Acad. Sci. U. S. A.* **2013**, *110* (32), 12936−12941.

(3) Hallquist, M.; Wenger, J. C.; Baltensperger, U.; Rudich, Y.; Simpson, D.; Claeys, M.; Dommen, J.; Donahue, N. M.; George, C.; Goldstein, A. H.; Hamilton, J. F.; Herrmann, H.; Hoffmann, T.; Iinuma, Y.; Jang, M.; Jenkin, M. E.; Jimenez, J. L.; Kiendler-Scharr, A.; Maenhaut, W.; McFiggans, G.; Mentel, T. F.; Monod, A.; Prevot, A. S. H.; Seinfeld, J. H.; Surratt, J. D.; Szmigielski, R.; Wildt, J. The formation, properties and impact of secondary organic aerosol: current and emerging issues. *Atmos. Chem. Phys.* **2009**, *9* (14), 5155−5236.

(4) Zhang, Q.; Worsnop, D. R.; Canagaratna, M. R.; Jimenez, J. L. Hydrocarbon-like and oxygenated organic aerosols in Pittsburgh: insights into sources and processes of organic aerosols. *Atmos. Chem. Phys.* **2005**, *5*, 3289−3311.

(5) Kesselmeier, J.; Staudt, M. Biogenic volatile organic compounds (VOC): An overview on emission, physiology and ecology. *J. Atmos. Chem.* **1999**, *33* (1), 23−88.

DOI: 10.1021/acs.est.5b03038
Environ. Sci. Technol. 2015, 49, 12242−12252

(6) Vutukuru, S.; Griffin, R. J.; Dabdub, D. Simulation and analysis of secondary organic aerosol dynamics in the South Coast Air Basin of California. *J. Geophys. Res.* **2006**, *111*, D10S12.
(7) Robinson, A. L.; Donahue, N. M.; Shrivastava, M. K.; Weitkamp, E. A.; Sage, A. M.; Grieshop, A. P.; Lane, T. E.; Pierce, J. R.; Pandis, S. N. Rethinking organic aerosols: Semivolatile emissions and photochemical aging. *Science* **2007**, *315* (5816), 1259−1262.
(8) Weber, R. J.; Sullivan, A. P.; Peltier, R. E.; Russell, A.; Yan, B.; Zheng, M.; de Gouw, J.; Warneke, C.; Brock, C.; Holloway, J. S.; Atlas, E. L.; Edgerton, E. A study of secondary organic aerosol formation in the anthropogenic-influenced southeastern United States. *J. Geophys. Res.-Atmos.* **2007**, *112*, D13302.
(9) Han, Y. M.; Iwamoto, Y.; Nakayama, T.; Kawamura, K.; Mochida, M. Formation and evolution of biogenic secondary organic aerosol over a forest site in Japan. *J. Geophys. Res.-Atmos.* **2014**, *119* (1), 259−273.
(10) Kourtchev, I.; Fuller, S. J.; Giorio, C.; Healy, R. M.; Wilson, E.; O'Connor, I.; Wenger, J. C.; McLeod, M.; Aalto, J.; Ruuskanen, T. M.; Maenhaut, W.; Jones, R.; Venables, D. S.; Sodeau, J. R.; Kulmala, M.; Kalberer, M. Molecular composition of biogenic secondary organic aerosols using ultrahigh-resolution mass spectrometry: comparing laboratory and field studies. *Atmos. Chem. Phys.* **2014**, *14* (4), 2155−2167.
(11) Putman, A. L.; Offenberg, J. H.; Fisseha, R.; Kundu, S.; Rahn, T. A.; Mazzoleni, L. R. Ultrahigh-resolution FT-ICR mass spectrometry characterization of alpha-pinene ozonolysis SOA. *Atmos. Environ.* **2012**, *46*, 164−172.
(12) Gao, S.; Keywood, M.; Ng, N. L.; Surratt, J.; Varutbangkul, V.; Bahreini, R.; Flagan, R. C.; Seinfeld, J. H. Low-molecular-weight and oligomeric components in secondary organic aerosol from the ozonolysis of cycloalkenes and alpha-pinene. *J. Phys. Chem. A* **2004**, *108* (46), 10147−10164.
(13) Muller, L.; Reinnig, M. C.; Hayen, H.; Hoffmann, T. Characterization of oligomeric compounds in secondary organic aerosol using liquid chromatography coupled to electrospray ionization Fourier transform ion cyclotron resonance mass spectrometry. *Rapid Commun. Mass Spectrom.* **2009**, *23* (7), 971−979.
(14) Kalberer, M.; Paulsen, D.; Sax, M.; Steinbacher, M.; Dommen, J.; Prevot, A. S. H.; Fisseha, R.; Weingartner, E.; Frankevich, V.; Zenobi, R.; Baltensperger, U. Identification of polymers as major components of atmospheric organic aerosols. *Science* **2004**, *303* (5664), 1659−1662.
(15) Hoffmann, T.; Bandur, R.; Marggraf, U.; Linscheid, M. Molecular composition of organic aerosols formed in the α-pinene/O_3 reaction: Implications for new particle formation processes. *J. Geophys. Res.* **1998**, *103* (D19), 25569−25578.
(16) Vaden, T. D.; Imre, D.; Beránek, J.; Shrivastava, M.; Zelenyuk, A. Evaporation kinetics and phase of laboratory and ambient secondary organic aerosol. *Proc. Natl. Acad. Sci. U. S. A.* **2011**, *108* (6), 2190−2195.
(17) Saleh, R.; Donahue, N. M.; Robinson, A. L. Time Scales for Gas-Particle Partitioning Equilibration of Secondary Organic Aerosol Formed from Alpha-Pinene Ozonolysis. *Environ. Sci. Technol.* **2013**, *47* (11), 5588−5594.
(18) Grieshop, A. P.; Donahue, N. M.; Robinson, A. L. Is the gas-particle partitioning in alpha-pinene secondary organic aerosol reversible? *Geophys. Res. Lett.* **2007**, *34*, L14810.
(19) Wilson, J.; Imre, D.; Beranek, J.; Shrivastava, M.; Zelenyuk, A. Evaporation Kinetics of Laboratory-Generated Secondary Organic Aerosols at Elevated Relative Humidity. *Environ. Sci. Technol.* **2015**, *49* (1), 243−249.
(20) Cappa, C. D.; Jimenez, J. L. Quantitative estimates of the volatility of ambient organic aerosol. *Atmos. Chem. Phys.* **2010**, *10* (12), 5409−5424.
(21) Cappa, C. D.; Wilson, K. R. Evolution of organic aerosol mass spectra upon heating: implications for OA phase and partitioning behavior. *Atmos. Chem. Phys.* **2011**, *11* (5), 1895−1911.
(22) Pathak, R. K.; Presto, A. A.; Lane, T. E.; Stanier, C. O.; Donahue, N. M.; Pandis, S. N. Ozonolysis of alpha-pinene: parameterization of secondary organic aerosol mass fraction. *Atmos. Chem. Phys.* **2007**, *7* (14), 3811−3821.
(23) Kolesar, K. R.; Chen, C.; Johnson, D.; Cappa, C. D. The influences of mass loading and rapid dilution of secondary organic aerosol on particle volatility. *Atmos. Chem. Phys.* **2015**, *15* (16), 9327−9343.
(24) Kroll, J. H.; Seinfeld, J. H. Chemistry of secondary organic aerosol: Formation and evolution of low-volatility organics in the atmosphere. *Atmos. Environ.* **2008**, *42* (16), 3593−3624.
(25) Karnezi, E.; Riipinen, I.; Pandis, S. N. Measuring the atmospheric organic aerosol volatility distribution: a theoretical analysis. *Atmos. Meas. Tech.* **2014**, *7*, 2953−2965.
(26) Atkinson, R.; Baulch, D. L.; Cox, R. A.; Crowley, J. N.; Hampson, R. F.; Hynes, R. G.; Jenkin, M. E.; Rossi, M. J.; Troe, J.; IUPAC Subcommittee. Subcommittee, I., Evaluated kinetic and photochemical data for atmospheric chemistry: Volume II - gas phase reactions of organic species. *Atmos. Chem. Phys.* **2006**, *6* (11), 3625−4055.
(27) Huffman, J. A.; Ziemann, P. J.; Jayne, J. T.; Worsnop, D. R.; Jimenez, J. L. Development and characterization of a fast-stepping/scanning thermodenuder for chemically-resolved aerosol volatility measurements. *Aerosol Sci. Technol.* **2008**, *42* (5), 395−407.
(28) Grieshop, A. P.; Miracolo, M. A.; Donahue, N. M.; Robinson, A. L. Constraining the Volatility Distribution and Gas-Particle Partitioning of Combustion Aerosols Using Isothermal Dilution and Thermodenuder Measurements. *Environ. Sci. Technol.* **2009**, *43* (13), 4750−4756.
(29) Saleh, R.; Shihadeh, A.; Khlystov, A. On transport phenomena and equilibration time scales in thermodenuders. *Atmos. Meas. Tech.* **2011**, *4* (3), 571−581.
(30) Emanuelsson, E. U.; Watne, A. K.; Lutz, A.; Ljungstrom, E.; Hallquist, M. Influence of Humidity, Temperature, and Radicals on the Formation and Thermal Properties of Secondary Organic Aerosol (SOA) from Ozonolysis of beta-Pinene. *J. Phys. Chem. A* **2013**, *117* (40), 10346−10358.
(31) Gloaguen, E.; Mysak, E. R.; Leone, S. R.; Ahmed, M.; Wilson, K. R. Investigating the chemical composition of mixed organic-inorganic particles by "soft" vacuum ultraviolet photoionization: The reaction of ozone with anthracene on sodium chloride particles. *Int. J. Mass Spectrom.* **2006**, *258* (1−3), 74−85.
(32) Chhabra, P. S.; Ng, N. L.; Canagaratna, M. R.; Corrigan, A. L.; Russell, L. M.; Worsnop, D. R.; Flagan, R. C.; Seinfeld, J. H. Elemental composition and oxidation of chamber organic aerosol. *Atmos. Chem. Phys.* **2011**, *11* (17), 8827−8845.
(33) Zhao, D. F.; Kaminski, M.; Schlag, P.; Fuchs, H.; Acir, I. H.; Bohn, B.; Haseler, R.; Kiendler-Scharr, A.; Rohrer, F.; Tillmann, R.; Wang, M. J.; Wegener, R.; Wildt, J.; Wahner, A.; Mentel, T. F. Secondary organic aerosol formation from hydroxyl radical oxidation and ozonolysis of monoterpenes. *Atmos. Chem. Phys.* **2015**, *15* (2), 991−1012.
(34) Lee, A.; Goldstein, A. H.; Keywood, M. D.; Gao, S.; Varutbangkul, V.; Bahreini, R.; Ng, N. L.; Flagan, R. C.; Seinfeld, J. H. Gas-phase products and secondary aerosol yields from the ozonolysis of ten different terpenes. *J. Geophys. Res.* **2006**, *111*, D07302.
(35) Herrmann, F.; Winterhalter, R.; Moortgat, G. K.; Williams, J. Hydroxyl radical (OH) yields from the ozonolysis of both double bonds for five monoterpenes. *Atmos. Environ.* **2010**, *44* (28), 3458−3464.
(36) Tolocka, M. P.; Jang, M.; Ginter, J. M.; Cox, F. J.; Kamens, R. M.; Johnston, M. V. Formation of oligomers in secondary organic aerosol. *Environ. Sci. Technol.* **2004**, *38* (5), 1428−1434.
(37) Kristensen, K.; Enggrob, K. L.; King, S. M.; Worton, D. R.; Platt, S. M.; Mortensen, R.; Rosenoern, T.; Surratt, J. D.; Bilde, M.; Goldstein, A. H.; Glasius, M. Formation and occurrence of dimer esters of pinene oxidation products in atmospheric aerosols. *Atmos. Chem. Phys.* **2013**, *13* (7), 3763−3776.
(38) Hall, W. A.; Johnston, M. V. Oligomer Formation Pathways in Secondary Organic Aerosol from MS and MS/MS Measurements with

DOI: 10.1021/acs.est.5b03038
Environ. Sci. Technol. 2015, 49, 12242−12252

High Mass Accuracy and Resolving Power. *J. Am. Soc. Mass Spectrom.* **2012**, *23* (6), 1097−1108.
(39) Ulbrich, I. M.; Canagaratna, M. R.; Zhang, Q.; Worsnop, D. R.; Jimenez, J. L. Interpretation of organic components from Positive Matrix Factorization of aerosol mass spectrometric data. *Atmos. Chem. Phys.* **2009**, *9* (9), 2891−2918.
(40) Chen, Q.; Li, Y. L.; McKinney, K. A.; Kuwata, M.; Martin, S. T. Particle mass yield from beta-caryophyllene ozonolysis. *Atmos. Chem. Phys.* **2012**, *12* (7), 3165−3179.
(41) Ng, N. L.; Kroll, J. H.; Chan, A. W. H.; Chhabra, P. S.; Flagan, R. C.; Seinfeld, J. H. Secondary organic aerosol formation from m-xylene, toluene, and benzene. *Atmos. Chem. Phys.* **2007**, *7* (14), 3909−3922.
(42) Salo, K.; Hallquist, M.; Jonsson, A. M.; Saathoff, H.; Naumann, K. H.; Spindler, C.; Tillmann, R.; Fuchs, H.; Bohn, B.; Rubach, F.; Mentel, T. F.; Muller, L.; Reinnig, M.; Hoffmann, T.; Donahue, N. M. Volatility of secondary organic aerosol during OH radical induced ageing. *Atmos. Chem. Phys.* **2011**, *11* (21), 11055−11067.
(43) Emanuelsson, E. U.; Mentel, T. F.; Watne, A. K.; Spindler, C.; Bohn, B.; Brauers, T.; Dorn, H. P.; Hallquist, A. M.; Haseler, R.; Kiendler-Scharr, A.; Muller, K. P.; Pleijel, H.; Rohrer, F.; Rubach, F.; Schlosser, E.; Tillmann, R.; Hallquist, M. Parameterization of Thermal Properties of Aging Secondary Organic Aerosol Produced by Photo-Oxidation of Selected Terpene Mixtures. *Environ. Sci. Technol.* **2014**, *48* (11), 6168−6176.
(44) An, W. J.; Pathak, R. K.; Lee, B. H.; Pandis, S. N. Aerosol volatility measurement using an improved thermodenuder: Application to secondary organic aerosol. *J. Aerosol Sci.* **2007**, *38* (3), 305−314.
(45) Pathak, R. K.; Salo, K.; Emanuelsson, E. U.; Cai, C. L.; Lutz, A.; Hallquist, A. M.; Hallquist, M. Influence of Ozone and Radical Chemistry on Limonene Organic Aerosol Production and Thermal Characteristics. *Environ. Sci. Technol.* **2012**, *46* (21), 11660−11669.
(46) Lee, B. H.; Pierce, J. R.; Engelhart, G. J.; Pandis, S. N. Volatility of secondary organic aerosol from the ozonolysis of monoterpenes. *Atmos. Environ.* **2011**, *45* (14), 2443−2452.
(47) Huffman, J. A.; Docherty, K. S.; Aiken, A. C.; Cubison, M. J.; Ulbrich, I. M.; DeCarlo, P. F.; Sueper, D.; Jayne, J. T.; Worsnop, D. R.; Ziemann, P. J.; Jimenez, J. L. Chemically-resolved aerosol volatility measurements from two megacity field studies. *Atmos. Chem. Phys.* **2009**, *9* (18), 7161−7182.
(48) Loza, C. L.; Coggon, M. M.; Nguyen, T. B.; Zuend, A.; Flagan, R. C.; Seinfeld, J. H. On the Mixing and Evaporation of Secondary Organic Aerosol Components. *Environ. Sci. Technol.* **2013**, *47* (12), 6173−6180.
(49) Emanuelsson, E. U.; Hallquist, M.; Kristensen, K.; Glasius, M.; Bohn, B.; Fuchs, H.; Kammer, B.; Kiendler-Scharr, A.; Nehr, S.; Rubach, F.; Tillmann, R.; Wahner, A.; Wu, H. C.; Mentel, T. F. Formation of anthropogenic secondary organic aerosol (SOA) and its influence on biogenic SOA properties. *Atmos. Chem. Phys.* **2013**, *13* (5), 2837−2855.
(50) Lambe, A. T.; Onasch, T. B.; Croasdale, D. R.; Wright, J. P.; Martin, A. T.; Franklin, J. P.; Massoli, P.; Kroll, J. H.; Canagaratna, M. R.; Brune, W. H.; Worsnop, D. R.; Davidovits, P. Transitions from Functionalization to Fragmentation Reactions of Laboratory Secondary Organic Aerosol (SOA) Generated from the OH Oxidation of Alkane Precursors. *Environ. Sci. Technol.* **2012**, *46* (10), 5430−5437.
(51) Offenberg, J. H.; Kleindienst, T. E.; Jaoui, M.; Lewandowski, M.; Edney, E. O. Thermal properties of secondary organic aerosols. *Geophys. Res. Lett.* **2006**, *33*, L03816.
(52) Maksymiuk, C. S.; Gayahtri, C.; Gil, R. R.; Donahue, N. M. Secondary organic aerosol formation from multiphase oxidation of limonene by ozone: mechanistic constraints via two-dimensional heteronuclear NMR spectroscopy. *Phys. Chem. Chem. Phys.* **2009**, *11* (36), 7810−7818.
(53) Bateman, A. P.; Nizkorodov, S. A.; Laskin, J.; Laskin, A. Time-resolved molecular characterization of limonene/ozone aerosol using high-resolution electrospray ionization mass spectrometry. *Phys. Chem. Chem. Phys.* **2009**, *11* (36), 7931−7942.
(54) Ehn, M.; Thornton, J. A.; Kleist, E.; Sipila, M.; Junninen, H.; Pullinen, I.; Springer, M.; Rubach, F.; Tillmann, R.; Lee, B.; Lopez-Hilfiker, F.; Andres, S.; Acir, I. H.; Rissanen, M.; Jokinen, T.; Schobesberger, S.; Kangasluoma, J.; Kontkanen, J.; Nieminen, T.; Kurten, T.; Nielsen, L. B.; Jorgensen, S.; Kjaergaard, H. G.; Canagaratna, M.; Dal Maso, M.; Berndt, T.; Petaja, T.; Wahner, A.; Kerminen, V. M.; Kulmala, M.; Worsnop, D. R.; Wildt, J.; Mentel, T. F. A large source of low-volatility secondary organic aerosol. *Nature* **2014**, *506* (7489), 476−479.
(55) Bonn, B.; Schuster, G.; Moortgat, G. K. Influence of water vapor on the process of new particle formation during monoterpene ozonolysis. *J. Phys. Chem. A* **2002**, *106* (12), 2869−2881.
(56) Mysak, E. R. Gentle photoionization of organic constituents using vacuum ultraviolet aerosol mass spectrometry. Ph.D. Dissertation, University of North Carolina at Chapel Hill, Chapel Hill, NC, 2006.
(57) Huffman, J. A.; Docherty, K. S.; Mohr, C.; Cubison, M. J.; Ulbrich, I. M.; Ziemann, P. J.; Onasch, T. B.; Jimenez, J. L. Chemically-Resolved Volatility Measurements of Organic Aerosol from Different Sources. *Environ. Sci. Technol.* **2009**, *43* (14), 5351−5357.
(58) Kostenidou, E.; Lee, B. H.; Engelhart, G. J.; Pierce, J. R.; Pandis, S. N. Mass Spectra Deconvolution of Low, Medium, and High Volatility Biogenic Secondary Organic Aerosol. *Environ. Sci. Technol.* **2009**, *43* (13), 4884−4889.
(59) Virtanen, A.; Joutsensaari, J.; Koop, T.; Kannosto, J.; Yli-Pirila, P.; Leskinen, J.; Makela, J. M.; Holopainen, J. K.; Poschl, U.; Kulmala, M.; Worsnop, D. R.; Laaksonen, A. An amorphous solid state of biogenic secondary organic aerosol particles. *Nature* **2010**, *467* (7317), 824−827.
(60) Abramson, E.; Imre, D.; Beranek, J.; Wilson, J.; Zelenyuk, A. Experimental determination of chemical diffusion within secondary organic aerosol particles. *Phys. Chem. Chem. Phys.* **2013**, *15* (8), 2983−2991.
(61) Renbaum-Wolff, L.; Grayson, J. W.; Bateman, A. P.; Kuwata, M.; Sellier, M.; Murray, B. J.; Shilling, J. E.; Martin, S. T.; Bertram, A. K. Viscosity of alpha-pinene secondary organic material and implications for particle growth and reactivity. *Proc. Natl. Acad. Sci. U. S. A.* **2013**, *110* (20), 8014−8019.
(62) Koop, T.; Bookhold, J.; Shiraiwa, M.; Poschl, U. Glass transition and phase state of organic compounds: dependency on molecular properties and implications for secondary organic aerosols in the atmosphere. *Phys. Chem. Chem. Phys.* **2011**, *13* (43), 19238−19255.
(63) Epstein, S. A.; Blair, S. L.; Nizkorodov, S. A. Direct Photolysis of α-Pinene Ozonolysis Secondary Organic Aerosol: Effect on Particle Mass and Peroxide Content. *Environ. Sci. Technol.* **2014**, *48* (19), 11251−11258.
(64) Epstein, S. A.; Riipinen, I.; Donahue, N. M. A Semiempirical Correlation between Enthalpy of Vaporization and Saturation Concentration for Organic Aerosol. *Environ. Sci. Technol.* **2010**, *44* (2), 743−748.
(65) Cappa, C. D. A model of aerosol evaporation kinetics in a thermodenuder. *Atmos. Meas. Tech.* **2010**, *3* (3), 579−592.
(66) Faulhaber, A. E.; Thomas, B. M.; Jimenez, J. L.; Jayne, J. T.; Worsnop, D. R.; Ziemann, P. J. Characterization of a thermodenuder-particle beam mass spectrometer system for the study of organic aerosol volatility and composition. *Atmos. Meas. Tech.* **2009**, *2* (1), 15−31.
(67) Yasmeen, F.; Vermeylen, R.; Szmigielski, R.; Iinuma, Y.; Boge, O.; Herrmann, H.; Maenhaut, W.; Claeys, M. Terpenylic acid and related compounds: precursors for dimers in secondary organic aerosol from the ozonolysis of alpha- and beta-pinene. *Atmos. Chem. Phys.* **2010**, *10* (19), 9383−9392.
(68) Claeys, M.; Iinuma, Y.; Szmigielski, R.; Surratt, J. D.; Blockhuys, F.; Van Alsenoy, C.; Boege, O.; Sierau, B.; Gomez-Gonzalez, Y.; Vermeylen, R.; Van der Veken, P.; Shahgholi, M.; Chan, A. W. H.; Herrmann, H.; Seinfeld, J. H.; Maenhaut, W. Terpenylic Acid and Related Compounds from the Oxidation of alpha-Pinene: Implications for New Particle Formation and Growth above Forests. *Environ. Sci. Technol.* **2009**, *43* (18), 6976−6982.

DOI: 10.1021/acs.est.5b03038
Environ. Sci. Technol. 2015, 49, 12242−12252

(69) Muller, L.; Reinnig, M. C.; Warnke, J.; Hoffmann, T. Unambiguous identification of esters as oligomers in secondary organic aerosol formed from cyclohexene and cyclohexene/α-pinene ozonolysis. *Atmos. Chem. Phys.* **2008**, *8* (5), 1423−1433.
(70) Lopez-Hilfiker, F. D.; Mohr, C.; Ehn, M.; Rubach, F.; Kleist, E.; Wildt, J.; Mentel, T. F.; Carrasquillo, A.; Daumit, K.; Hunter, J.; Kroll, J. H.; Worsnop, D.; Thornton, J. A. Phase partitioning and volatility of secondary organic aerosol components formed from a-pinene ozonolysis and OH oxidation: the importance of accretion products and other low volatility compounds. *Atmos. Chem. Phys.* **2015**, *15* (14), 7765−7776.
(71) Docherty, K. S.; Wu, W.; Lim, Y. B.; Ziemann, P. J. Contributions of organic peroxides to secondary aerosol formed from reactions of monoterpenes with O3. *Environ. Sci. Technol.* **2005**, *39* (11), 4049−4059.
(72) Jaoui, M.; Lewandowski, M.; Docherty, K.; Offenberg, J. H.; Kleindienst, T. E. Atmospheric oxidation of 1,3-butadiene: characterization of gas and aerosol reaction products and implications for PM2.5. *Atmos. Chem. Phys.* **2014**, *14* (24), 13681−13704.
(73) Bilde, M.; Barsanti, K. C.; Booth, M.; Cappa, C. D.; Donahue, N. M.; Emanuelsson, E. U.; McFiggans, G.; Krieger, U. K.; Marcolli, C.; Topping, D.; Ziemann, P. J.; Barley, M.; Clegg, S. L.; Dennis-Smither, B. J.; Hallquist, M.; Hallquist, A. M.; Khlystov, A.; Kulmala, M.; Mogensen, D.; Percival, C. J.; Pope, F. D.; Reid, J. P.; Ribeiro da Silva, M. A. V.; Rosenoern, T.; Salo, K.; Soonsin, V.; Yli-Juuti, T.; Prisle, N. L.; Pagels, J.; Rarey, J.; Zardini, A. A.; Riipinen, I. Saturation Vapor Pressures and Transition Enthalpies of Low-Volatility Organic Molecules of Atmospheric Relevance: From Dicarboxylic Acids to Complex Mixtures. *Chem. Rev.* **2015**, *115*, 4115−4156.
(74) Shrivastava, M.; Zelenyuk, A.; Imre, D.; Easter, R.; Beranek, J.; Zaveri, R. A.; Fast, J. Implications of low volatility SOA and gas-phase fragmentation reactions on SOA loadings and their spatial and temporal evolution in the atmosphere. *J. Geophys. Res.-Atmos.* **2013**, *118* (8), 3328−3342.
(75) Carlton, A. G.; Bhave, P. V.; Napelenok, S. L.; Edney, E. D.; Sarwar, G.; Pinder, R. W.; Pouliot, G. A.; Houyoux, M. Model Representation of Secondary Organic Aerosol in CMAQv4.7. *Environ. Sci. Technol.* **2010**, *44* (22), 8553−8560.

DOI: 10.1021/acs.est.5b03038
Environ. Sci. Technol. 2015, 49, 12242−12252